AAPS PharmSciTech, Vol. 15, No. 4, August 2014 (© 2014)
DOI: 10.1208/s12249-014-0134-7

Research Article

A Comparison of Granules Produced by High-Shear and Fluidized-Bed Granulation Methods

Garett Morin[1] and Lauren Briens[1,2]

Received 16 December 2013; accepted 24 April 2014; published online 17 May 2014

Abstract. Placebo granules were manufactured by both wet high-shear and fluidized-bed techniques. The granules were compared based on size, shape, surface morphology, and a variety of different flowability measurements. This comparison showed that granule formation and growth were different, with induction growth for high-shear granulation and steady growth for fluidized-bed granulation. Final granules from high-shear granulation were more spherical and dense compared with the irregular granules from fluidized-bed granulation. The high-shear granules demonstrated better overall flow properties.

KEY WORDS: flowability; fluidized-bed granulation; granule characteristics; high-shear granulation.

INTRODUCTION

Granulation is a process that gathers small particles into a larger mass with the original particles still identifiable (1). In wet granulation, a process widely used in the pharmaceutical industry to agglomerate the active ingredient(s) and excipients, a liquid binder is sprayed onto the particles as they are agitated, usually in a high-shear mixer or fluidized bed. The particles are agglomerated with the liquid binder, by a combination of capillary and viscous forces until more permanent bonds are formed by drying. Granulation prevents segregation of the constituents of the powder mixture, improves the flow characteristics of the mixture, and improves compaction into a tablet.

In fluidized-bed granulation, the powder bed is maintained in a fluidized state by a flow of air injected upward through a distributor plate at the base of the granulator. Escape of the granulation material is prevented by exhaust filters, which can be periodically agitated to reintroduce material into the bed. The liquid binder is sprayed through a nozzle onto the top of the bed or through a draft tube inserted near the bed bottom. Granules form from adhesion of solid particles to the liquid droplets (2). The flow of fluidizing air creates continuous partial drying throughout the granulation process. Sufficient liquid is sprayed to produce granules of the required size, usually between approximately 150 and 600 μm, at which point the spray is stopped and the granules continue to dry in the fluidizing airstream. Fluidized-bed granulators have many advantages over high-shear mixing: all the granulation processes, including drying, are performed within the same apparatus. After high-shear granulation, the wet granules must be dried either through vacuum or microwave drying within the granulator or, more commonly, using a fluidized-bed dryer. The consolidation of granulation and drying using a fluidized-bed granulator then saves labor cost, transfer losses, and time. Furthermore, once the conditions affecting the granulation have been optimized, the process can be fully automated. However, a fluidized-bed granulator is initially expensive and the optimization of the process and product parameters requires extensive developmental work during initial formulation, scale-up, and production. Similar developmental work for high-shear granulation is not as extensive due to the smaller number of operational parameters and their interactions.

In high-shear granulation, the unmixed dry powders are placed in a mixing bowl usually containing an impeller, which revolves on a horizontal plane, and a chopper, which rotates either in the vertical or horizontal plane. The dry powders are mixed by the rotating impeller before the liquid binder is sprayed onto the top of the bed of powder. Agitation is maintained by the rotating impeller. As the liquid droplets disperse throughout the powder, they form granule nuclei. The granules grow until a predetermined optimum endpoint is reached. The granules are then usually transferred to another piece of equipment for drying, such as a fluidized-bed dryer. An advantage of high-shear granulation is that the process is completed within a short period of time. It does, however, need to be carefully controlled as the formulation can quickly progress from under- to overgranulated.

Both high-shear and fluidized-bed granulation processes exhibit the four key rate processes that contribute to granulation, as originally described by Ennis (3): wetting and nucleation, coalescence, consolidation, and attrition. Although these rate mechanisms can occur simultaneously in all processes, certain mechanisms may dominate and be more pronounced within each method. For instance, fluidized-bed granulators are strongly influenced by the wetting and nucleation process, whereas the mechanical dispersion of binding liquid by the impeller and chopper diminish the wetting

[1] Biomedical Engineering, The University of Western Ontario, London, CanadaN6A 5B9.
[2] To whom correspondence should be addressed. (e-mail: lbriens@uwo.ca)

contributions to granule size in high-shear operations. Consequently, granule consolidation is far more pronounced in high-shear mixing than fluidized-bed granulation.

Although there is a lot of published literature on high-shear granulation and fluidized-bed granulation, there is little documentation directly comparing the two processes. Table I provides a summary of the major studies that have directly compared high-shear and fluidized-bed granulations.

Flore *et al.* (9) compared a variety of granulations for a polymeric powder, including fluidized-bed and high-shear granulations. They used an Eirich R02 batchwise laboratory scale mixer operated at 1,500 rpm for the high-shear granulations and a conical laboratory scale bed for the fluidized-bed granulations. It was found that granules in the appropriate size range, 0.3–1 mm, could be prepared with both methods. The high-shear process resulted in a strong caking of the wet product in the mixing vessel. The methods produced granules with different morphologies: the fluidized-bed process produced porous particles with a fluffy, irregular appearance while the high-shear granules were more spherical. From dissolution tests, it was determined that both dissolved at similar rates, with the fluidized-bed granules dissolving only slightly faster. Finally, the high-shear granules had a much higher bulk density (400–500 g/cm^3) compared with that of the fluidized-bed granules (250–290 g/cm^3).

Agnese *et al.* (4) compared high-shear and fluidized-bed processes using aqueous PVP solutions and PVA-PEG graft copolymer. High-shear granules were denser as a result of higher mechanical stress applied during the process, whereas the fluidized-bed granules had a high porosity and less spherical particle shape. In terms of size distribution, coarser agglomerates with fewer fines were produced using high-shear granulation, whereas the size distribution was much narrower from the fluidized-bed process. N'Dri Stempfer *et al.* (5) also reported a narrower size distribution of granules from a fluidized bed compared with a high-shear granulation. They granulated using a Diosna P1/6 high-shear mixer at a speed of 200 rpm for both the impeller and chopper and a GEA Strea 1 fluidized bed.

Hausman (7) performed high-shear granulations in a Diosna VAC20 unit with an impeller speed of 150 rpm and a chopper speed of 3,000 rpm while fluidized-bed granulations were performed in a Glatt GPCG-5 unit utilizing top spray. In contrast to other researchers, Hausman (7) reported a narrower size distribution of granules from the high-shear rather than from the fluidized-bed granulation. The fluidized-bed granules, however, had a high mean diameter. Both the bulk and tapped densities of the fluidized-bed granules were lower than those from the high-shear granulation.

Gao *et al.* (6) conducted fluidized-bed granulations in a Niro MP-1, varying inlet temperature, inlet air flow, binder spray rate, and atomizing air pressure. High-shear granulations were completed in a Gral 10 L unit, using an experimentally optimized process with drying in a Glatt WSG-3 fluid bed dryer. The atomizing air pressure and spray rate of the binder solution during the fluidized-bed granulation affected granule size distribution while the inlet air flow rate had almost no effect. The bulk density and mean particle diameter for the fluidized-bed granules were significantly smaller than for granules prepared by the high-shear method. The high-shear process, however, produced granules with better flow properties and a higher compressibility, as described by Carr's index. The difference in granule compressibility was attributed to lower granule porosity as visualized in images taken by scanning electron microscope (SEM): granules from the high-shear granulation were more spherical and denser with fewer fines while the fluidized-bed granules were more loosely agglomerated, irregular in shape, and appeared to be more porous.

Research presented in the literature comparing high-shear and fluidized-bed granulation processes focuses on the comparison of granule shape, size, density, and porosity. Variations in reported granule properties may be attributed to formulations or differences in granulation equipment and process parameters. The effect of the granulation method on granule flowability has only been reported by Gao *et al.* (6) using the Carr index. A thorough study on the effect on flowability, specifically using dynamic measurements, has not yet been reported. The objective of this research was therefore to compare high-shear and fluidized-bed granulations using a placebo formulation through examination of the granulation mechanism and physical properties of the granules with a focus on dynamic flowability. For successful downstream operations, flowability of the granules is critical and dynamic measurements can provide valuable information for these operations.

MATERIALS AND METHODS

Product Formulation

A placebo formulation consisting of 50 wt.% lactose monohydrate (Merck), 45 wt.% microcrystalline cellulose (FMC Biopolymer Avicel PH 101), 4 wt.% hydroxypropyl

Table I. Summary of Literature Directly Comparing High-Shear and Fluidized-Bed Granules

	Mean size	Size distribution	Granule shape	Granule porosity	Bulk/tapped density	Flowability	Reference
High shear			Spherical		High		Flore *et al.* (9)
Fluidized bed			Irregular		Low		
High shear		Wide	Spherical	Low			Agnese *et al.* (4)
Fluidized bed		Narrow	Irregular	High			
High shear	Small	Narrow			High		Hausman *et al.* (7)
Fluidized bed	Large	Wide			Low		
High shear		Wide					N'Dri Stempfer
Fluidized bed		Narrow					*et al.* (5)
High shear	Large		Spherical	Low	High	Good	Gao *et al.* (6)
Fluidized bed	Small		Irregular	High	Low	Poor	

methylcellulose (Shin-Etsu Pharmacoat 603), and 1 wt.% croscarmellose sodium (Alfa Aesar) was used for all the trials.

High-Shear Granulation

All high-shear granulations were performed in a Fielder PMA-1 (GEA Pharma Systems, UK) high-shear granulator shown schematically in Fig. 1. The impeller and chopper were operated without binder addition for the first 2 min of each trial to mix the dry powder. A dry mass of 1.5 kg was used for each trial; this mass was within the optimum range of operation for this granulator. The impeller and chopper speeds were constant for all trials at 700 and 1,000 rpm, respectively. These parameters were previously identified as providing a large fraction of optimal granules (8).

At 2 min, binder addition was started with distilled water at 24°C as the liquid binder. The water was sprayed at a rate of approximately 46 g/min into the granulator using a nozzle left of center. Binder spraying continued for the entire specified wetting time for a trial. An optimal endpoint of 10 min, corresponding to a granule moisture content of about 31 wt.%, was previously identified (8). Trials, therefore, were conducted for different time intervals up to 10 min wetting to examine the progress of granulation.

Granules from each trial were spread out in a thin layer onto trays and oven dried at 24°C and a relative humidity of 2 to 3% for more than 24 h to ensure a granule moisture content of less than 2 wt.%. The dried granules were then immediately analyzed for various characteristics.

Fluidized-Bed Granulation

All fluidized-bed granulations were performed in a custom-made top-spray conical fluidized bed shown schematically in Fig. 2. A dry mass of 1.0 kg was used for each trial; this mass was within the optimum range of operation for this granulator. The fluidizing air velocity was constant for each trial at 0.95 or 1.35 m/s and at a relatively low temperature and humidity of 20°C and 15%, respectively.

The bed was first fluidized for 5 min to mix the dry powder. Binder addition was then started with distilled water at 24°C as the liquid binder. The water was sprayed at a rate of approximately 52 g/min at an atomization pressure of 0.7 bar into the granulator using a centered top-spray nozzle. The

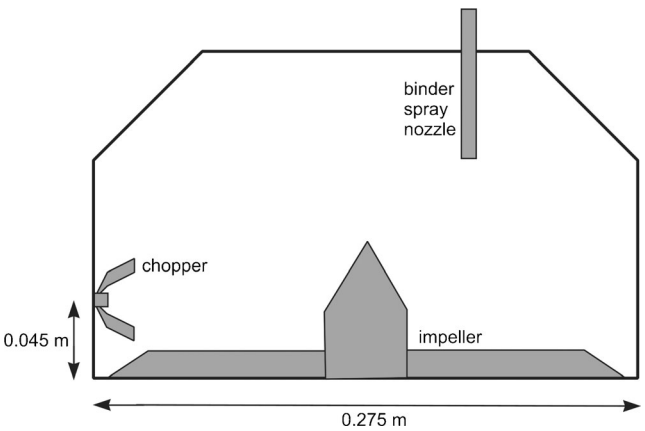

Fig. 1. Schematic diagram of the high-shear PMA-1 granulator

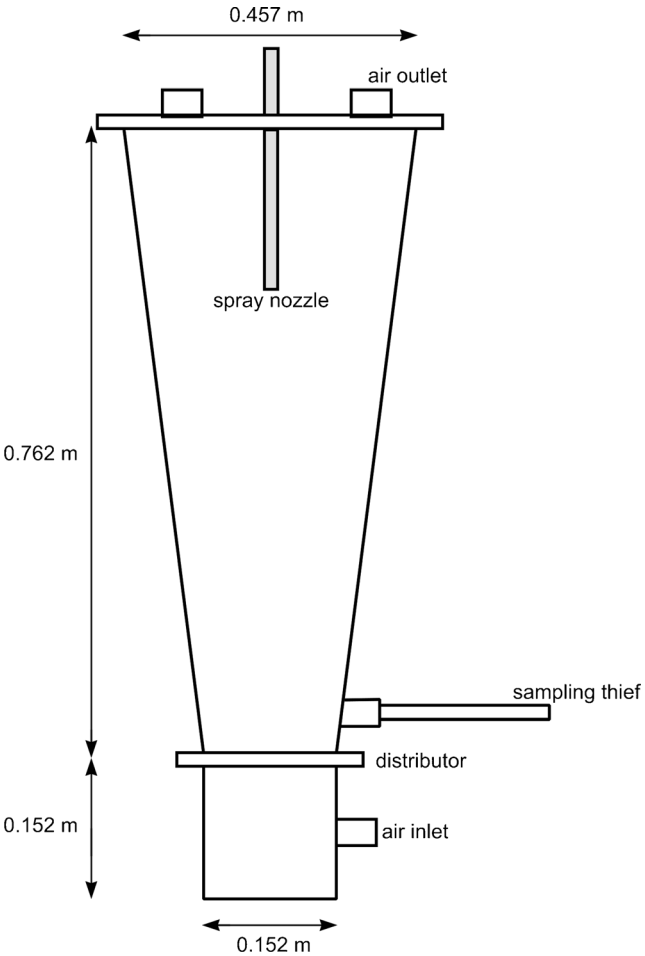

Fig. 2. Schematic diagram of the fluidized-bed granulator

spraying continued for the entire specified wetting time for a trial. At a fluidizing air velocity of 0.95 m/s, trials at time intervals up to 11 min or 37 wt.% moisture content were conducted. At 1.35 m/s fluidizing air velocity, trials continued until 13 min wetting time. The extra drying from the higher air flow, however, only resulted in a maximum granule moisture content of 31 wt.%.

Although the granules could remain in the fluidized bed to be dried, to better compare this granulation with the high-shear method, the granules were removed and tray dried. Granules from each trial were spread out in a thin layer onto trays and oven dried at 24°C and a relative humidity of 2 to 3% for more than 24 h to ensure a granule moisture content of less than 2 wt.%. The dried granules were then immediately analyzed for various characteristics.

Granule Analysis

Granule moisture content was determined through loss on drying at 105°C using a MettlerToledo HG63 halogen moisture analyzer. Duplicate samples of 5.0 g were analyzed.

Particle size analysis of the granules was performed through sieving using a Retsch AS200 vibratory sieve shaker at an amplitude of 0.01 mm and a frequency of 60 Hz for 30 min. For the analysis, 18 mesh cuts using standard sized stainless steel sieves ranging from 38 to 3,350 μm were used.

SEM images of the granules were taken using a Hitachi S4500 field emission SEM. The granules were mounted on a plate and coated with gold before examination. The images allowed the composition, shape and morphology of the granules to be examined and also for approximate comparison of size measurements from the sieving.

The bulk and tapped density of the particulates was measured using 100 mL samples. For the bulk density measurements, the powder flowed down a vibrating chute into a 100-mL cylinder and the mass of the powder sample within the cylinder was then measured:

$$\text{bulk density}\left(\frac{\text{g}}{\text{mL}}\right) = \frac{\text{mass of sample}}{100\ \text{mL}} \quad (1)$$

The sample within the cylinder was then vibrated/tapped, and the resulting volume was measured to determine the tapped density:

$$\text{tapped density}\left(\frac{\text{g}}{\text{mL}}\right) = \frac{\text{mass of sample}}{\text{tapped density volume(mL)}} \quad (2)$$

Duplicate density measurements were performed. The bulk and tapped density measurements then allowed the Carr index to be calculated:

$$\text{Carr index} = \frac{\text{tapped density} - \text{bulk density}}{\text{tapped density}} \times 100\% \quad (3)$$

Static angle of repose measurements were performed using a Powder Research Ltd. Angle of Repose Device. Samples of approximately 60 mL flowed down a vibrating chute and then through a funnel to form a pile below on a calibrated level platform to allow the angle of repose to be easily determined. Samples were measured in triplicate.

Various indicators of flowability were investigated using a Mercury Scientific Revolution Powder Analyzer. A sample size of 118 cm^3 was loaded into a drum with a diameter of 11 cm and width of 3.5 cm. This drum was rotated at 0.3 rpm until 128 avalanches had occurred, with an avalanche defined as being a rearrangement of at least 0.65 vol.% of the sample in the drum. The analyzer uses an optical technique with a resolution of 648×488 at 60 frames/s to monitor the behavior of the powder surface as the sample is rotated. Samples were measured in triplicate.

RESULTS

Figure 3 shows scanning electron micrograph images of the individual components of the formulation. Lactose monohydrate particles are large, angular, almost rectangular, and have a smooth surface morphology while microcrystalline cellulose particles are irregular fibers. Hydroxypropyl methylcellulose particles are also irregular fibers but very small and only present at 4 wt.% in the formulation, which made it difficult to detect in any agglomerates. The croscarmellose sodium comprised only 1 wt.% of the formulation and, as it is water soluble, it dissolved into the water binder and did not appear in images of any agglomerates.

Optimum granules were defined to have a diameter between 150 and 600 μm, be approximately spherical in shape and incorporate all components of the formulation. Fines were considered as particulates with diameters less than 150 μm while oversized granules were larger than 600 μm in diameter. To focus on granule properties, scanning electron images from each trial were taken from samples sieved to include only particles sized between 150 and 600 μm. Figure 4 shows scanning electron images of the 150 to 600 μm samples from the high-shear granulation trials. The granulation nuclei appeared to be primarily microcrystalline cellulose. After approximately 7–8 min, when the granule moisture content was about 20%, lactose monohydrate began to be incorporated into the nuclei. Further granulation created larger, more dense, and spherical granules. Figures 5 and 6 show scanning electron images of the 150 to 600 μm samples from the fluidized-bed granulation trials. In contrast to the high-shear results, nuclei from the fluidized-bed granulations appeared to be loose agglomerates of lactose monohydrate coated by microcrystalline cellulose fibers. As the granulation proceeded, granules grew in size but remained very porous and nonspherical.

The visual differences in porosity of the granules indicated in the scanning electron images were reflected in the dynamic densities shown in Fig. 7. High-shear granules increased the density of the formulation from 0.5 to about 0.57 g/mL while the granules from the fluidized bed had very low densities of about 0.3 g/mL.

Figure 8 shows that the Sauter mean diameter varied with granulation type and fluidizing velocity. For the high-shear granulation, significant growth did not occur until a critical moisture content of about 20 wt.%. Fluidized-bed granulation at 0.95 m/s also showed only minimal increases in the Sauter mean diameter until 20 wt.%. By contrast, size increases were steady, but only reached a maximum of about 225 μm at 25 wt.% moisture content for fluidized-bed granulation at 1.35 m/s.

The size distributions shown in Fig. 9 also show differences between the types of granulation. The minimal growth until a moisture content of 20 wt.% is observed for the high-shear granulation. More continuous growth was observed for the fluidized-bed granulations especially at a fluidization velocity of 1.35 m/s. The most favorable distribution of the maximum amount of optimum granules with minimal fines and oversized agglomerates was achieved with fluidized-bed granulation at 1.35 m/s. The lower fluidization velocity produced too many oversized agglomerates while the high-shear granulation started to rapidly overgranulate near a moisture content of 30 wt.%.

As particle size affects flowability and tabletability, the differential size distributions at granule moisture contents near 20 wt.% and then just below 30 wt.% were compared in Fig. 10. The size distributions were all narrow at the lower moisture content, but at the higher moisture content the fluidized-bed granulations created a wider size distribution with more large agglomerates than the high-shear granulation.

As shown in Fig. 11 for the Carr index, the high-shear granulation achieved the lowest index. Similar values were obtained for the fluidized-bed granulation at 0.95 m/s. For

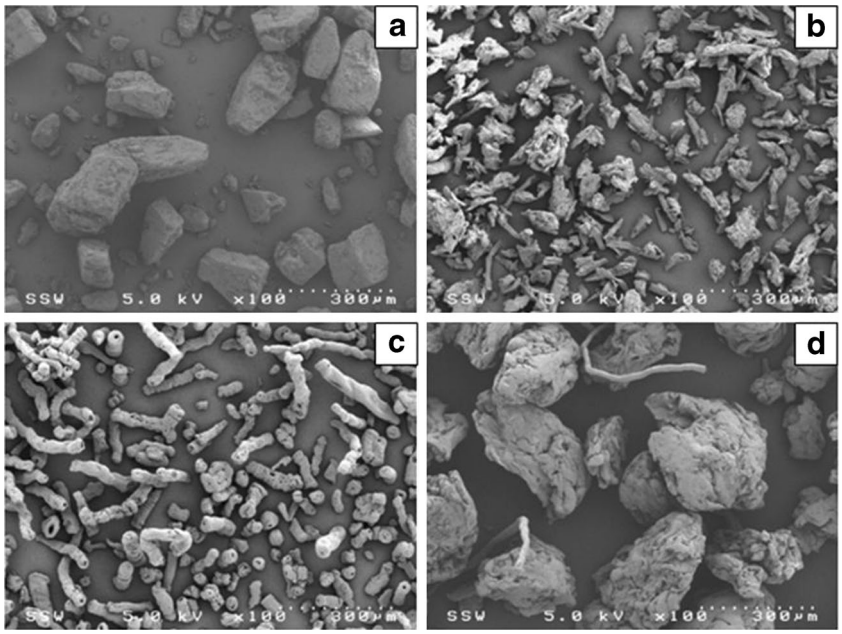

Fig. 3. Scanning electron micrograph images of the individual components of the formulation consisting of **a** lactose monohydrate, **b** microcrystalline cellulose, **c** hydroxypropyl methylcellulose, and **d** croscarmellose sodium

the fluidized-bed granulation at 1.35 m/s, however, the Carr index only decreased to about 20.

The static angle of repose, shown in Fig. 12, showed that the ungranulated formulation was very cohesive and exhibited poor flowability. The static angle of repose decreased for both types of granulations due to the increase in particle sizes from forming granules. The static angle of repose decreased to approximately 28° for the high-shear granulation and decreased to 27° for the fluidized-bed granulations indicating that the flowability was excellent for both the fluidized-bed granules and high-shear granules.

The avalanche curvature, shown in Fig. 13 indicates the curvature of the powder surface just before an avalanche. The avalanche curvature decreased as granules formed. Near the end of the processes, the avalanche curvature values were similar for both types of granulations.

The surface fractal, shown in Fig. 14, indicates the roughness of the powder surface as it avalanches. The surface fractal

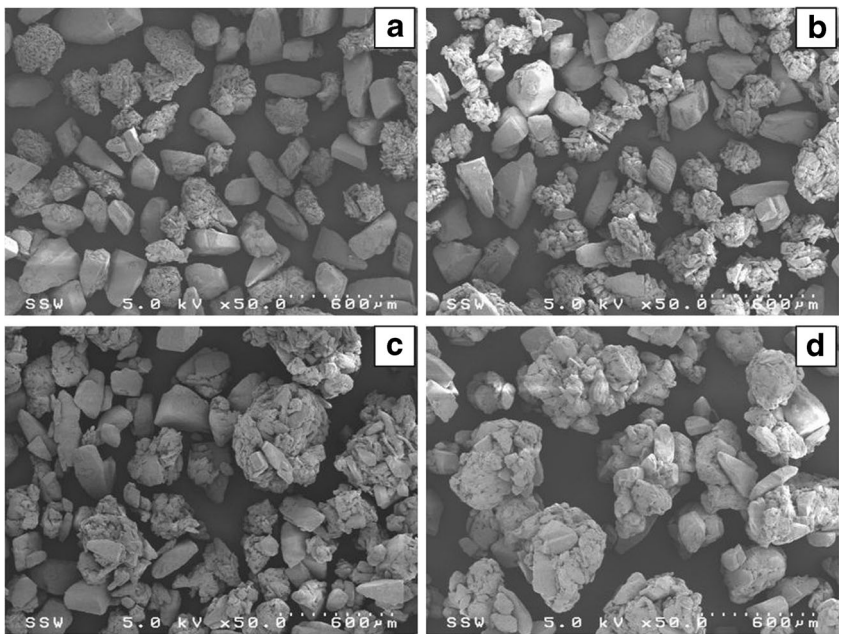

Fig. 4. Scanning electron images of samples from the high-shear granulation trials with **a** 20.0, **b** 26.0, **c** 30.2, and **d** 33.2 wt.% moisture content

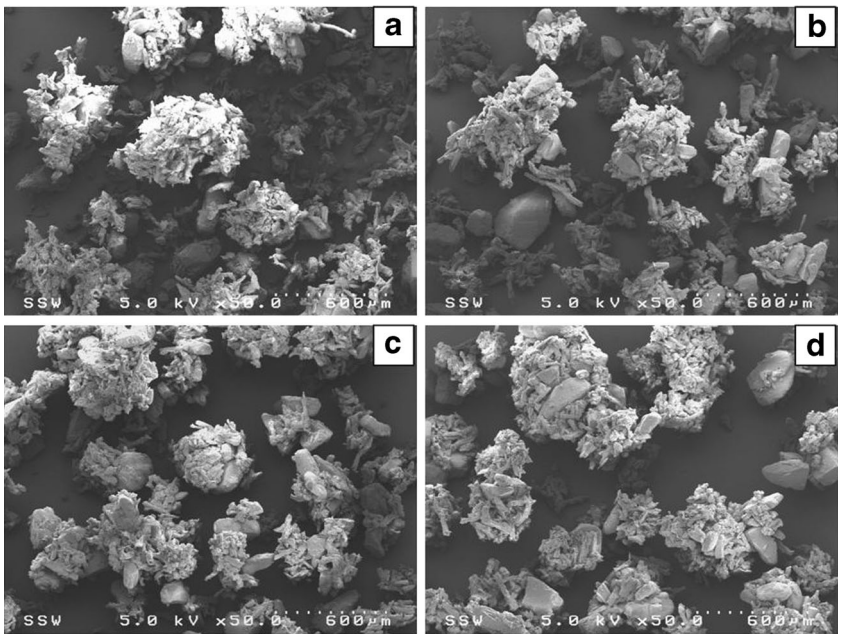

Fig. 5. Scanning electron images of samples from the fluidized-bed granulation trials at 0.95 m/s with **a** 11.5, **b** 19.9, **c** 29.9, and **d** 36.6 wt.% moisture content

of the fluidized-bed granulations reached a very high value of 10 while the high-shear granulations only reached a value of 7.

DISCUSSION

The scanning electron images of the samples taken from the granulations indicated that the formation of granule nuclei was different for the high-shear and fluidized-bed granulations. For the high-shear granulation, nuclei contained only microcrystalline cellulose. The powders were mixed for 2 min before liquid binder addition. During this dry mixing stage, the powders segregated: larger lactose particles were forced towards the sides and the bottom of the bowl while the microcrystalline cellulose fibers segregated to the middle of the bowl and near the top of the powder bed. As a result, primarily microcrystalline cellulose fibers were initially exposed to the binder spray. These hygroscopic fibers easily absorbed the binder and formed nuclei (8). For the fluidized-bed granulations, the nuclei consisted primarily of lactose monohydrate particles with a few attached microcrystalline cellulose fibers. Fluidization of the dry powders was difficult: lactose monohydrate requires high air velocities as it is a large

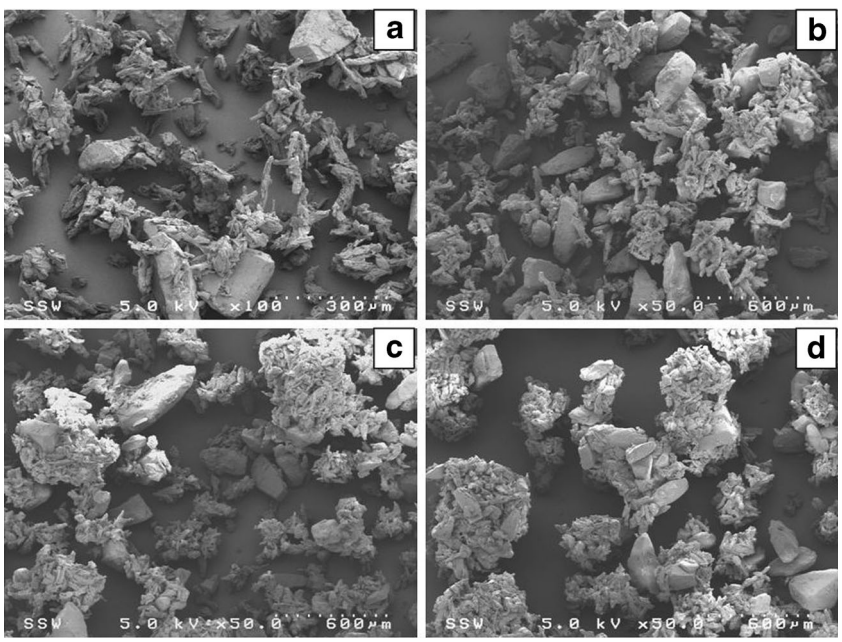

Fig. 6. Scanning electron images of samples from the fluidized-bed granulation trials at 1.35 m/s with **a** 12.0, **b** 16.8, **c** 20.7, and **d** 26.8 wt.% moisture content

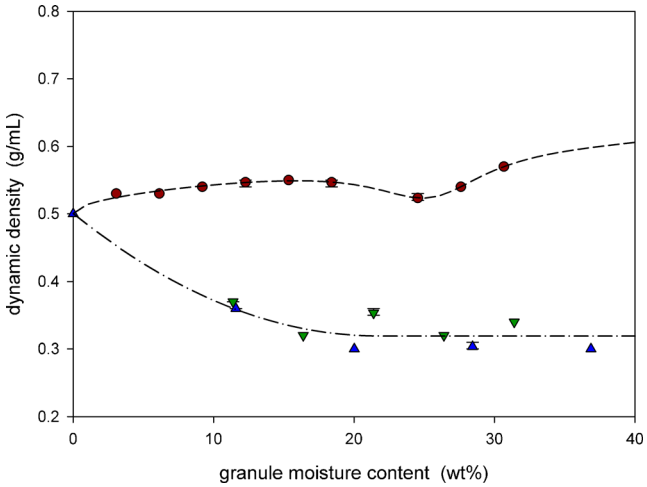

Fig. 7. Dynamic densities of granulation trials

particle, but the smaller microcrystalline cellulose also does not fluidize easily due to the fiber shape of the particles. The initial fluidization of the powders therefore did not promote segregation of the microcrystalline cellulose to the top of the bed to be overexposed to the liquid binder spray. Liquid binder was absorbed by the microcrystalline cellulose, but also coated the surface of the lactose monohydrate particles. Collisions between a wetted lactose monohydrate and microcrystalline cellulose resulted in nuclei that included both particles.

The scanning electron images (Fig. 4) combined with the particle size analysis (Fig. 9) indicated that the granule growth mechanism was different for the two types of granulation. For the high-shear granulation, granule formation followed the induction growth mechanism: growth remained minimal until a moisture content of about 20 wt.% and then increased rapidly. At this critical moisture content of 20 wt.%, densification forced the water in the microcrystalline cellulose nuclei to the surface of these agglomerates making the surface more adhesive. Subsequent collisions with lactose monohydrate particles allowed the formation of liquid bridges resulting in granules with microcrystalline cellulose and lactose monohydrate. Further collisions incorporated more lactose

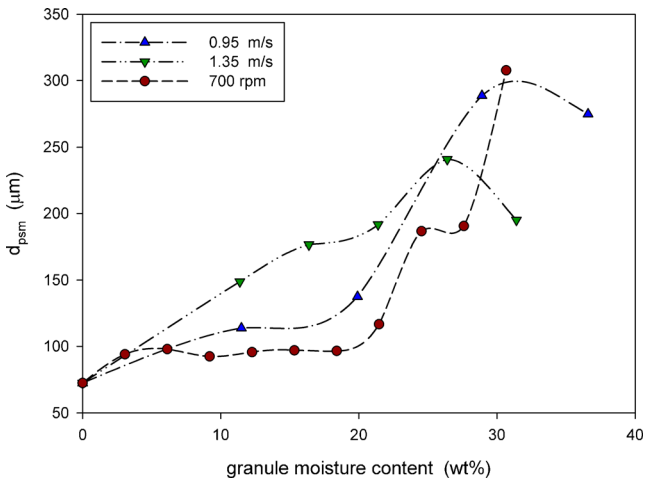

Fig. 8. Sauter mean diameters of granulation trials

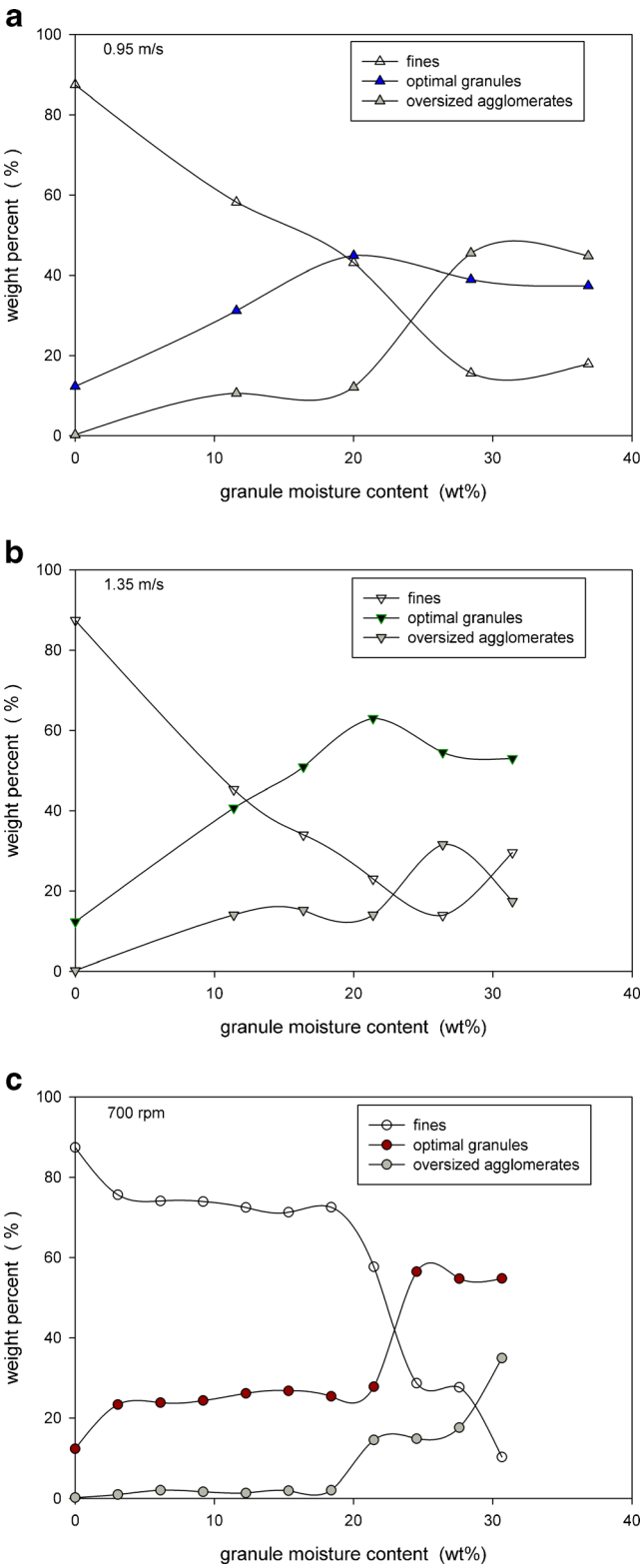

Fig. 9. Size distributions of granulation trials

monohydrate into the granules and then granule consolidation and coalescence promoted further growth. The high-shear forces from the impeller promoted the formation of spherical granules with low porosity. For the fluidized-bed granulations, granule formation followed a slow

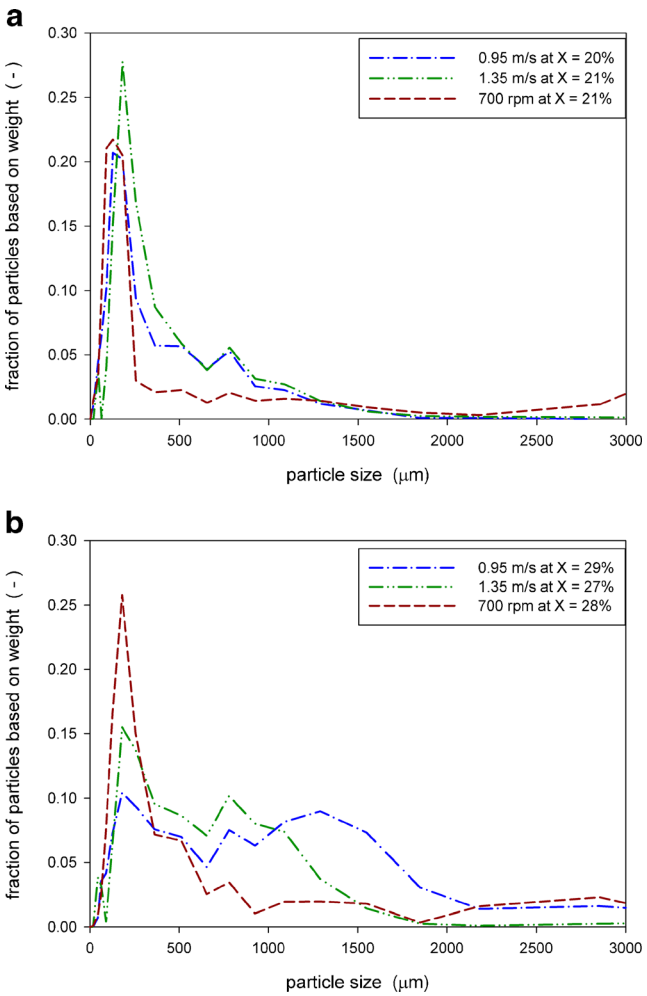

Fig. 10. Differential size distributions of granulation trials at **a** moisture content near 20 wt.% and **b** moisture content near 30 wt.%

but steady growth mechanism. Granule growth occurred through coalescence of nuclei and smaller granules as the binder continued to be sprayed onto the bed. As only low shear forces are present in the fluidized bed, the granules were irregularly shaped and highly porous. At larger granule sizes, this structure becomes particularly susceptible to attrition as shown by the decrease in agglomerates and increase in fines near the end of the granulation. The differences in the granule shape and porosity were consistent with the reported literature (4–6,9).

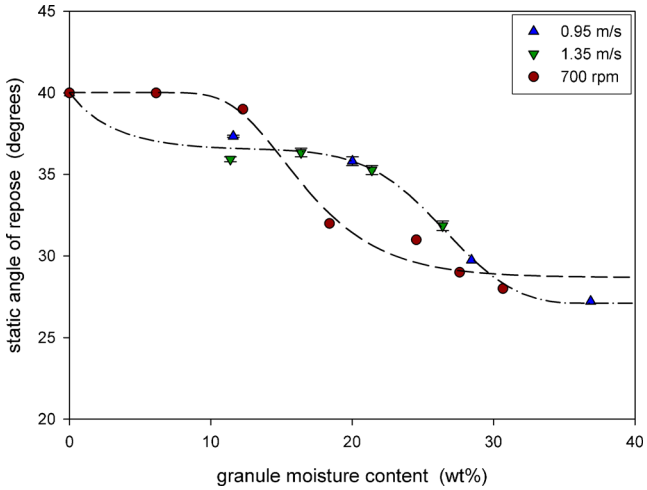

Fig. 12. Static angle of repose of granulation trials

Comparing the size distributions from the granulations was difficult as the different growth mechanisms meant that the progress varied with the type of granulation. Comparison using granule moisture content as a basis (Fig. 10) showed that, at lower moisture levels, the size distributions for all the granulations were narrow. Differences between the granulations were larger at a higher moisture level just below 30 wt.%: the size distribution for the high-shear granulation remained narrow while the distribution widened to include larger sizes for the fluidized-bed granulations. At even higher moisture levels, it would be expected that the size distribution of the high-shear granulation would widen as the formation of oversized agglomerates occurred while the distribution for the fluidized-bed granulations would not change significantly as any larger agglomerates would be fragile due to their irregular shape and high porosity and therefore minimized through breakage and attrition.

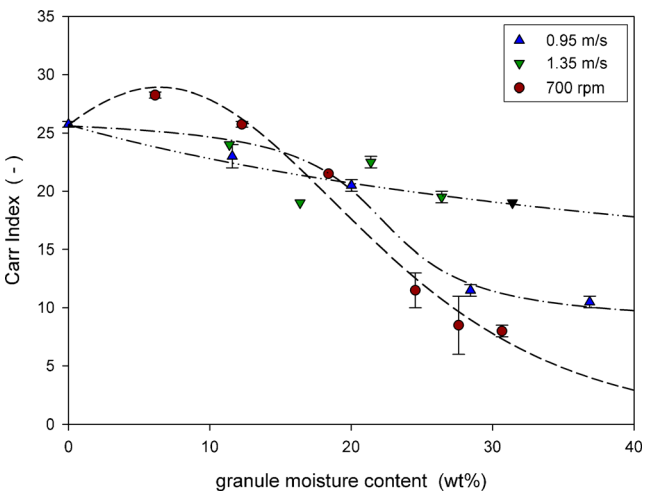

Fig. 11. Carr index of granulation trials

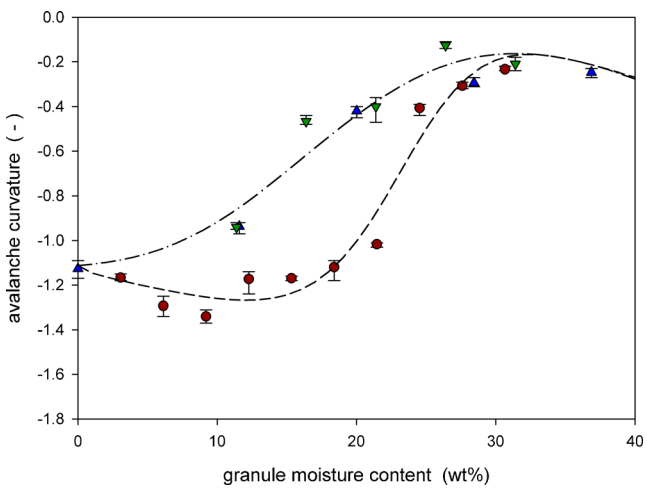

Fig. 13. Avalanche curvature of granulation trials

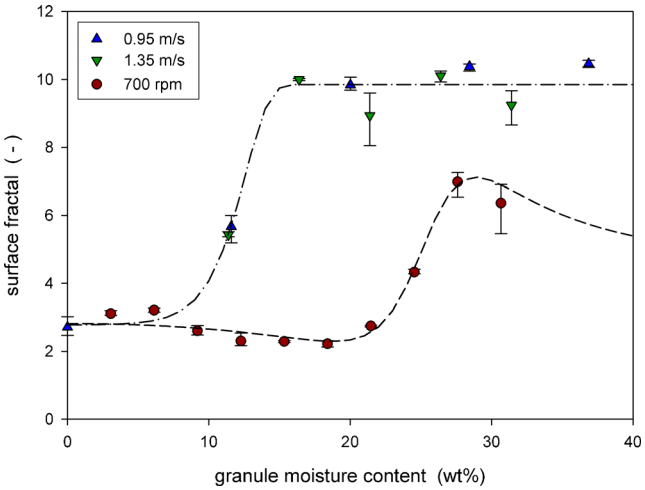

Fig. 14. Surface fractal of granulation trials

In the literature, the size distribution results have varied. Hausman (7) showed a wider distribution for fluidized bed compared with high-shear granulations while others (4,10,11) have reported the reverse with large agglomerates from the high-shear granulation contributing to its wide size distribution. Different procedures were used for the granulations including liquid binder spray rate and processing time. The stopping point for each process therefore may have occurred at different stages in the granulation contributing to the differences in the size distribution results.

The dynamic densities, measured using the revolution analyzer, were much lower for the fluidized-bed granules than for the high-shear granules: 0.32 to 0.42 g/mL from fluidized-bed granulation *versus* 0.59 g/mL from high-shear granulation. These densities were comparable to the bulk densities obtained by Gao *et al.* (6), who attributed the density differences to granule size, size distribution, shape, and porosity. Density is a critical parameter for tableting. For the same tablet die, a low density could result in a tablet with a weight below an acceptable level and the tablet must then be discarded.

The flow properties of the granulations manufactured by the two methods are important to compare and assess the appropriateness of each to produce a tablet with specified properties. Granule size, size distribution and shape and density are critical factors affecting flowability. Each flowability measurement is affected by these factors differently and therefore many measurements must be examined to provide a complete assessment of flowability.

The Carr index indicates both compressibility and flowability. A Carr index below 15 indicates low compressibility but good flow properties while a value above 25 indicates a very compressible powder with very poor flow (5). As expected, the lowest Carr index of 8 was obtained by the high-shear granulation reflecting the dense and spherical granules. The high density of the granules limits further compressibility while the density and shape combined contribute to improved flowability. The Carr index of granules obtained from the fluidized-bed granulations ranged from 10 to about 20 as the fluidizing velocity was increased from 0.95 to 1.35 m/s. The higher Carr index for the fluidized-bed granulations reflects the porous granules, which would be compressible. These lighter density and nonspherical granules, however, may have some flow difficulties. The range in the Carr index for the fluidized-bed granulation trials reflects the differences in the size distributions with larger granules, which would exhibit better flow properties, obtained for the trials at the lower fluidization velocity. Gao *et al.* (6) reported similar Carr index values: 13 for granules from high-shear granulation and 15 to 26 for granules from fluidized-bed granulation with the different process parameters affecting the values.

The static angle of repose also indicates flowability. As shown in Fig. 12, both types of granulation decreased the static angle of repose indicating improved flowability. The static angle of repose measurements, however, did not provide sufficient resolution to identify small changes in flowability. Therefore, differences in flowability due to the granulation methods were difficult to detect from these measurements.

The avalanche curvature indicates the curvature of the powder surface just before an avalanche. A linear surface would have a curvature equal to zero. A concave surface, which would form with a cohesive powder that would accumulate at the drum perimeter before avalanching, would have a negative curvature. The avalanche curvature therefore shows that the formulation was initially very cohesive and that granulation improved the flowability. The improvement occurred at lower moisture content for the fluidized-bed granulation reflecting the earlier granule growth compared with the high-shear granulation. Near the end of the granulations, the avalanche curvature indicated similar flowability potential for both types of granulations. The Carr index, however, showed differences between the granulations as it indicated both flowability and compressibility together in the one index.

A fractal value close to one indicates a smooth and even surface, measured by the moving powder in the Revolution Analyzer. The powder surface affects tablet die filling as the powder must flow well and then become evenly distributed within the die. The surface fractal values are closest to one at the beginning of the granulation. Although flowability is poor at this low moisture content and the sample powder surface is concave, the fractal value is low and the actual surface is smooth due to the small size of the particles. As the granulation progresses, the surface fractal increased reflecting the formation of the granules and the disruption of the smooth surface by these larger particles. The surface fractal of the fluidized-bed granulations reached a very high value of 10 while the high-shear granulations only reached a value of 7. This variation reflected the large and irregular particles obtained with the fluidized-bed granulations.

CONCLUSIONS

A lactose-based placebo formulation was granulated using both high-shear and fluidized-bed methods. The results indicated differences in the formation and then subsequent growth of the granules from the two methods. Differences in the granule nuclei formation result from particle segregation within the high-shear granulator compared with flow patterns within the fluidized bed, which provide different exposure to the liquid binder spray. The differences in granule nuclei combined with flow and shear levels led to induction growth for the high-shear granulation, but steady state growth for the fluidized bed.

Although the composition of the granules was the same for both types of granulations, the properties of the granules

were different, leading to variations in flowability. No one parameter can quantify the difference in flowability between high-shear bed fluidized-bed granules. Each parameter measures a different property of the granules, contributing to the overall flowability of the mixture. Examination of many parameters then led to the overall conclusion that the high-shear granules exhibit better flow properties than granules produced by the fluidized bed. Many granule properties are important and must be considered for successful downstream tabletting processes. One of these properties is flowability. High-shear granules, therefore, may be easier to use during tabletting.

ACKNOWLEDGMENTS

The authors would like to acknowledge the support of the Natural Sciences and Engineering Research Council of Canada (NSERC) as well as the Ontario Graduate Scholarship (OGS) for their financial support. The University of Western Ontario Graduate Thesis Research Award Fund (GTRAF) is also acknowledged for financial contribution.

REFERENCES

1. Ennis B. Design & optimization of granulation processes for enhanced product performance. Nashville: E&G Associates; 1990.
2. Faure A, York P, Rowe R. Process control and scale-up of pharmaceutical wet granulation processes: a review. Eur J Pharm Biopharm. 2001;52:269–77.
3. Ennis B, Litster J. Particle size enlargement. Perry's chemical engineer's handbook. 7th ed. New York: McGraw-Hill; 1997. p. 20–89.
4. Agnese T, Cech T, Geiselhart V, Wagner E. Comparing the wet granulation properties of PVA-PEG graft copolymer and different PVP grades in fluid bed granulation processes applying different inlet air temperatures. Aix en Provence: 2nd Conference on Innovation in Drug Deliver; 2010.
5. N'Dri-Stempfer B, Oulahna D, Eterradossi O, Benhassaine A, Dodds J. Binder granulation and compaction of coloured powders. Powder Tech. 2003;130:247–52.
6. Gao JZH, Jain A, Motheram R, Gray D, Hussain M. Fluid bed granulation of a poorly water soluble, low density, micronized drug: comparison with high shear granulation. Int J Pharm. 2002;237:1–14.
7. Hausman DS. Comparison of low shear, high shear, and fluid bed granulation during low dose tablet process development. Drug Dev Ind Pharm. 2004;30:259–66.
8. Briens L, Logan R. The effect of the chopper on granules from wet high-shear granulation using a PMA-1 granulator. AAPS PharmSciTech. 2011;12(4):1358–65.
9. Flore K, Schoenherr M, Feise H. Aspects of granulation in the chemical industry. Powder Tech. 2009;189:327–31.
10. Murakami H, Yoneyama T, Nakajima K, Kobayashi M. Correlation between loose density and compactibility of granules prepared by various granulation methods. Int J Pharm. 2001;216:159–64.
11. Stahl H. Comparing different granulation techniques. Pharm Tech Eur. 2004;16(11):23–7.